Construction of an l-Tyrosine Chassis in Pichia pastoris Enhances Aromatic Secondary Metabolite Production from Glycerol

Kumokita, Ryota ; Bamba, Takahiro ; Inokuma, Kentaro ; Yoshida, Takanobu ; Ito, Yoichiro ; Kondo, Akihiko ; Hasunuma, Tomohisa

(Citation)
ACS Synthetic Biology,11(6):2098-2107

(Issue Date)
2022-06-17

(Resource Type)
journal article

(Version)
Accepted Manuscript

TITLE: Construction of an L-Tyrosine chassis in *Pichia pastoris* enhances aromatic secondary metabolites production from glycerol

AUTHORS:

Ryota Kumokita, Takahiro Bamba, Kentaro Inokuma, Takanobu Yoshida, Yoichiro Ito, Akihiko Kondo, Tomohisa Hasunuma*

ABSTRACT

Bioactive plant-based secondary metabolites such as stilbenoids, flavonoids, and benzylisoquinoline alkaloids (BIAs) are produced from L-Tyrosine (L-Tyr) and have a wide variety of commercial applications. Therefore, building a microorganism with high L-Tyr productivity (L-Tyr chassis) is of immense value for large scale production of various aromatic compounds. The aim of this study was to develop an L-Tyr chassis in the non-conventional yeast *Pichia pastoris* (*Komagataella phaffii*) to produce various aromatic secondary metabolites (resveratrol, naringenin, norcoclaurine, and reticuline). Overexpression of feedback-inhibition insensitive variants of 3-deoxy-D-arabino-heptulosonate-7-phosphate synthase ($ARO4^{K229L}$) and chorismate mutase ($ARO7^{G141S}$) enhanced L-Tyr titer from glycerol in *P. pastoris*. These engineered *P. pastoris* strains increased the titer of resveratrol, naringenin, and norcoclaurine by 258%, 244%, and 3400%, respectively after expressing the corresponding heterologous pathways. The titer of resveratrol and naringenin further increased by 305% and 249% resulting in yields of 1825 mg/L and 1067 mg/L, respectively in fed-batch fermentation which is the highest titer from glycerol reported to date. Furthermore, the resveratrol-producing strain accumulated intermediates in the shikimate pathway. L-Tyr-derived aromatic compounds were produced using crude glycerol by-product from biodiesel fuel (BDF) production. Constructing L-Tyr chassis is a promising strategy to increase the titer of various aromatic secondary metabolites and *P. pastoris* is an attractive host for high

yield production of L-Tyr-derived aromatic compounds from glycerol.

GRAPHICAL ABSTRACT

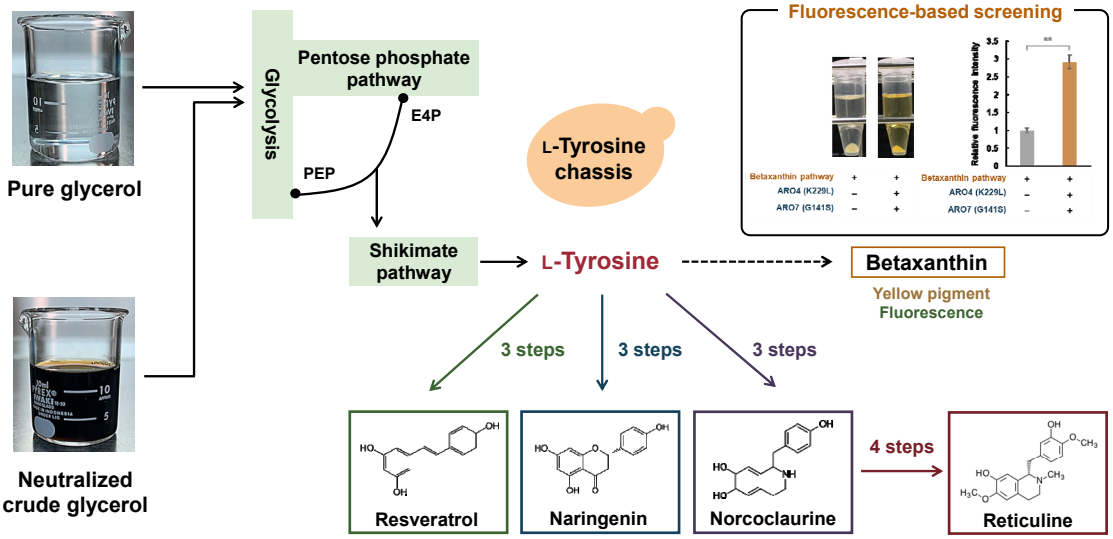

KEYWORDS

aromatic secondary metabolite, L-Tyrosine chassis, *Pichia pastoris*, non-conventional yeast, metabolomics, crude glycerol

INTRODUCTION

Plant-derived aromatic compounds are widely used as pharmaceutical drugs, dietary supplements, and nutraceuticals[1-3]. The production of these compounds predominantly relies on costly and inefficient extraction methods from low productivity plants[4-6]. Chemosynthesis does not improve productivity because of the complicated processes, strict reaction conditions, and poor selectivity[7,8]. Microbial production with reconstituted plant biosynthetic pathways has received increasing attention to ensure a sustainable supply of useful aromatic compounds and meet future anticipated demands[9,10].

The aromatic amino acid L-Tyrosine (L-Tyr) is a building block to produce stilbenoids, flavonoids, and benzylisoquinoline alkaloids (BIAs) in many plants. Thus, optimization of L-Tyr supply is important for producing L-Tyr-derived aromatic compounds in quantities that compete with commercial demands[11] and engineering microorganisms for L-Tyr overproduction is extensively studied[12-14]. For example, *Saccharomyces cerevisiae* has been genetically engineered for aromatic compound production[15-17]. Although *S. cerevisiae* is the preferred host due to its robustness and high stress tolerance during fermentation[12], repression of ethanol production to produce aromatic compounds in high yield is difficult[18]. Hence, exploring alternative yeast platforms is of immense value.

The metabolism of Crabtree-negative yeasts such as *Yarrowia lipolytica* and *Pichia pastoris* (*Komagataella phaffii*) does not divert carbon flux to ethanol, and carbon partitioning among the various pathways is well balanced[14]. Recently, the yield of aromatic compounds using *Y. lipolytica* greatly increased compared to that of *S. cerevisiae*[19,20] suggesting productivity differs among microbial hosts. *P. pastoris* is widely used as a chassis to produce heterologous proteins for research and industrial purposes[21,22] which does not produce fermentative by-products under aerobic conditions because its glycolytic flux does not exceed the respiratory capacity[23,24]. Glycerol is

63 often used as a carbon source during *P. pastoris* fermentation because it encodes four
64 H^+/glycerol symporters in its genome allowing for efficient metabolism and high
65 biomass productivity[24-26]. Glycerol requires fewer enzymatic reactions for the
66 biosynthesis of phosphoenolpyruvate (PEP) from glycolysis and erythrose-4-phosphate
67 (E4P) from the pentose phosphate pathway (PPP) compared to glucose (Figure 1). PEP
68 and E4P are essential precursors for L-Tyr biosynthesis.

69 In this study, an L-Tyr chassis was developed in *P. pastoris* by rational
70 engineering to increase the titer of various L-Tyr-derived aromatic secondary
71 metabolites. Initial screening utilized a simple betaxanthin fluorescence assay to search
72 for the overexpression of target genes enhancing L-Tyr titer. The potential of the L-Tyr
73 chassis to produce resveratrol, naringenin, norcoclaurine, and reticuline from glycerol
74 was investigated by co-expressing the required heterologous pathways (Figure 1).
75 Furthermore, the metabolic responses of the engineered resveratrol-producing strains
76 were investigated and the potential of *P. pastoris* to produce aromatic secondary
77 metabolite from crude glycerol by-product of biodiesel fuel (BDF) was evaluated.
78

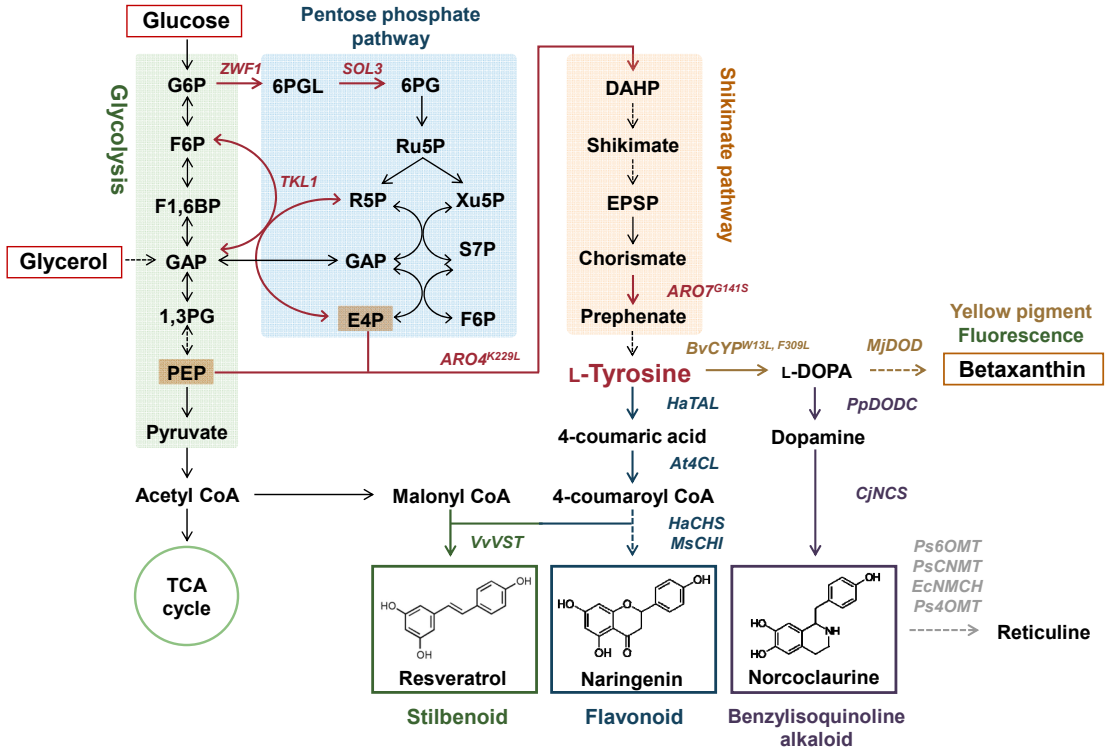

Figure 1. Biosynthetic pathway of betaxanthin, resveratrol, naringenin, norcoclaurine, and reticuline in *P. pastoris*. The native pathway in *P. pastoris* is represented by black and red arrows. The red arrow represents the overexpression of genes. The pathways to produce betaxanthin, resveratrol, naringenin, norcoclaurine, and reticuline are illustrated in yellow, green, blue, purple, and gray, respectively. The dashed arrows indicate multiple enzymatic steps. G6P: glucose-6-phosphate; F6P: fructose-6-phosphate; F1,6BP: fructose-1,6-bisphosphate; GAP: glyceraldehyde 3-phosphate; 1,3PG: 1,3-bisphosphoglycerate; PEP: phosphoenolpyruvate; 6PGL: 6-phosphogluconolactone; 6PG: 6-phosphogluconate; Ru5P: ribulose-5-phosphate; R5P: ribose-5-phosphate; Xu5P: xylulose-5-phosphate; S7P: sedoheptulose-7-phosphate; E4P: erythrose-4-phosphate; TCA cycle: tricarboxylic acid cycle; DAHP: 3-deoxy-D-arabinoheptulosonate 7-phosphate; EPSP: 5-*O*-(1-carboxyvinyl)-3-phosposhikimate; ZWF1: glucose-6-phosphate dehydrogenase from *P. pastoris*; SOL3: 6-phosphogluconolactonase from *P. pastoris*; TKL1: transketolase from *P. pastoris*; $ARO4^{K229L}$: DAHP synthase (K229L) from

Saccharomyces cerevisiae; ARO7^{G141S}: chorismate mutase (G141S) from *S. cerevisiae*; BvCYP$^{W13L, F903}$: Tyrosine hydroxylase (W13L, F903L) from *Beta vulgaris*; MjDOD: DOPA dioxygenase from *Mirabilis jalapa*; PpDODC: DOPA decarboxylase from *Pseudomonas putida*; CjNCS: norcoclaurine synthase from *Coptis japonica*; HaTAL: Tyrosine ammonia-lyase from *Herpetosiphon aurantiacus*; At4CL: 4-coumarate CoA ligase from *Arabidopsis thaliana*; VvVST: resveratrol synthase from *Vitis vinifera*; HaCHS: chalcone synthase from *Hypericum androsaemum*; MsCHI: chalcone isomerase from *Medicago sativa*; Ps6OMT: 6-*O*-methyltransferase from *Papaver somniferum*; PsCNMT: coclaurine *N*-methyltransferase from *P. somniferum*; EcNMCH: *N*-methylcoclaurine hydroxylase from *Eschscholzia californica*; Ps4OMT: 4'-*O*-methyltransferase from *P. somniferum*.

RESULTS

Identification of optimal engineering based on betaxanthin fluorescence

To search for overexpression target genes that contribute to enhance the L-Tyr titer in a high-throughput manner, we employed betaxanthin production pathway (Figure 1). Betaxanthin is an L-Tyr-derived yellow pigment emitting green fluorescence used to evaluate the strength of metabolic flux to L-Tyr. An engineered *P. pastoris* strain (CD strain) expressing the betaxanthin pathway was generated by introducing tyrosine hydroxylase from *Beta vulgaris* (*BvCYP$^{W13L, F309L}$*) and DOPA dioxygenase from *Mirabilis jalapa* (*MjDOD*) to detect L-Tyr production (Figure 1) and identify target genes contributing to enhanced L-Tyr titer in a high-throughput manner. The yellow coloration and green fluorescence of CD strain indicated successful betaxanthin production (Figure 2, Supporting Figure S1). We targeted PPP and shikimate pathway genes to improve L-Tyr titer. In *S. cerevisiae*, transketolase (*TKL1*), feedback-inhibition insensitive variants of 3-deoxy-D-arabino-heptulosonate-7-phosphate synthase (*ARO4^{K229L}*) and chorismate mutase (*ARO7^{G141S}*) were common overexpression targets

to increase the titer of L-Tyr-derived aromatic compounds[11,12]. Overexpression of 6-gluconolactonase (*SOL3*) and glucose-6-phosphate dehydrogenase (*ZWF1*) has been reported to enhance the flux to PPP in *P. pastoris*[27]. In this study, overexpression of *TKL1*, *SOL3*, and *ZWF1* from *P. pastoris*, and/or *ARO4*^{K229L} and *ARO7*^{G141S} from *S. cerevisiae* were introduced, respectively (Figure 1) using the CD strain (Table 1).

Measurement of fluorescence intensity in the engineered *P. pastoris* strains indicated that overexpression of *TKL1*, *SOL3*, and *ZWF1* from the PPP pathway did not have a statistically significant effect ($p > 0.05$) on betaxanthin levels while overexpression of *ARO4*^{K229L} and *ARO7*^{G141S} from the shikimate pathway in strain CD47m enhanced betaxanthin fluorescence by 191% (Figure 2). However, expression of these genes from both the PPP and shikimate pathways produced less betaxanthin fluorescence than the CD47m strain (Figure 2). Therefore, overexpression of *ARO4*^{K229L} and *ARO7*^{G141S} was employed to increase the titer of L-Tyr-derived aromatic compounds in subsequent experiments.

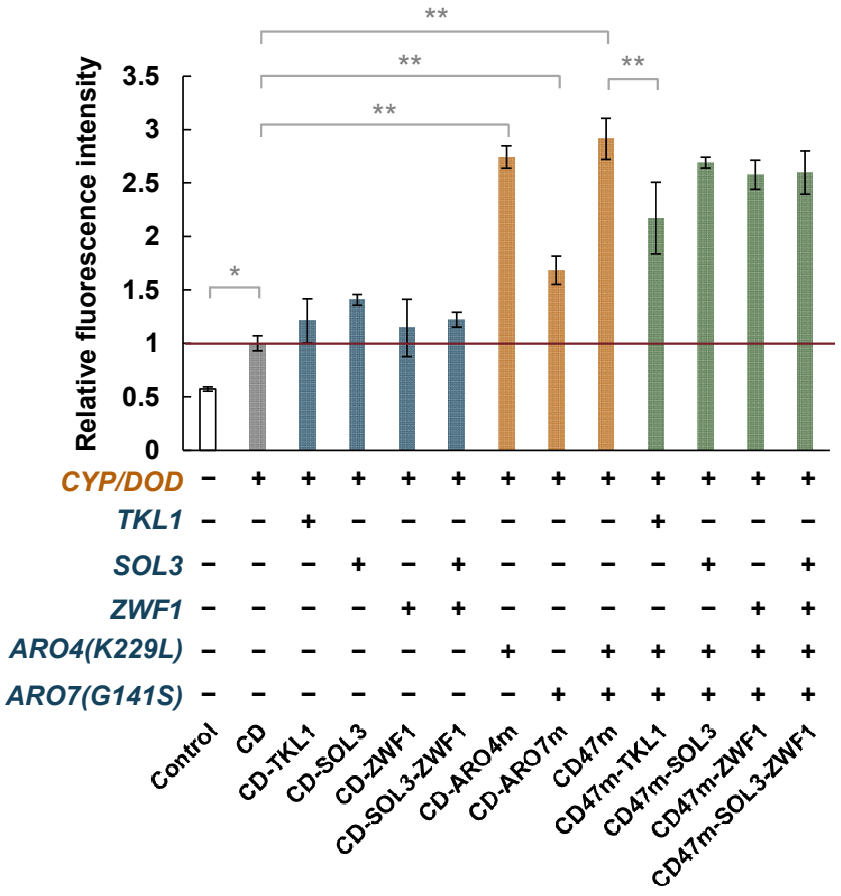

Figure 2. Betaxanthin fluorescence. Relative fluorescence intensity of the CD strain expressing pentose phosphate pathway (PPP) genes (blue), shikimate pathway genes (orange), and both PPP and shikimate pathway genes (green) after 24 h incubation in YPG medium. Error bars represent the standard deviation of three independent biological samples. The strains used in this study are summarized in Table 1. Control: *P. pastoris* CBS7435 *Δdnl4 Δhis4*; *CYP*, *DOD*, *TKL1*, *SOL3*, *ZWF1*, $ARO4^{K229L}$, and $ARO7^{G141S}$ as stated in Figure 1. Statistical analysis was performed using EZR (two-tailed, two-sample unequal variance; $*p < 0.05$, $**p < 0.005$).

Resveratrol production from glycerol

Downstream L-Tyr products resveratrol, naringenin, and norcoclaurine were tested in the following sections to determine if they are positively affected by increased L-Tyr production (Figure 1). A resveratrol-producing strain (T4V strain) was developed through the introduction of *Herpetosiphon aurantiacus* (*HaTAL*), 4-coumarate CoA ligase from *Arabidopsis thaliana* (*At4CL*), and stilbene synthase from *Vitis vinifera* (*VvVST*)[28] into a parent strain (*P. pastoris* CBS7435 *Δdnl4 Δhis4*). Furthermore, $ARO4^{K229L}$ and $ARO7^{G141S}$ were co-overexpressed to produce the T4V-ARO47m strain. The T4V-ARO47m strain was slightly defective in cell growth (Supporting Figure S2) and produced 451 mg/L resveratrol compared with 126 mg/L for the T4V strain with a yield of 22.5 mg/g-glycerol consumed (Figure 3A). Resveratrol titer in the T4V-ARO47m strain was further tested using fed-batch fermentation in a jar fermenter (Figure 3B) with constant DO and pH levels, and feeding solution added at the specified time. Cell growth (OD_{600}) plateaued after 72 h of fermentation, while the resveratrol titer continuously increased and reached 1825 mg/L with a yield of 16.6 mg/g-glycerol consumed after 120 h of fermentation which is an improvement of 305% compared to cultivation in flasks (Figure 3B) and is the highest resveratrol titer from glycerol reported to date (Supporting Table S1).

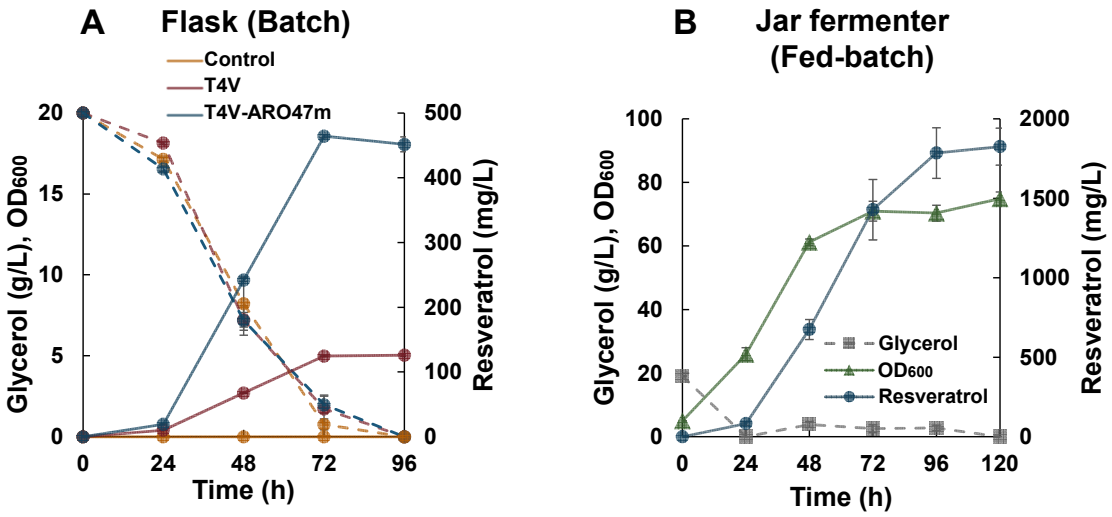

Figure 3. Resveratrol production in engineered *P. pastoris* strains. (A) Time course of resveratrol production and glycerol consumption in YPG culture medium of resveratrol-producing strains (T4V and T4V-ARO47m) and their parent strain CBS7435 *Δdnl4 Δhis4* (Control). Error bars represent standard deviations of three independent biological samples. The solid lines and dashed lines represent the resveratrol titer and glycerol concentration, respectively. (B) Fed-batch fermentation of the T4V-ARO47m strain in the jar fermenter. The feed was added from 24 to 96 h. Error bars represent the standard deviation of two independent biological samples.

Quantification of intracellular metabolites in engineered *P. pastoris* strains

To investigate the metabolic responses by overexpressing $ARO4^{K229L}$ and $ARO7^{G141S}$ in *P. pastoris*, the intracellular metabolites of the T4V, T4V-ARO47m, and their parent strain (*P. pastoris* CBS7435 *Δdnl4 Δhis4*) were extracted and quantified. There was no difference in the accumulation of glycolysis and PPP compounds at the beginning of glycerol consumption (24 h fermentation), except for an accumulation of fructose-1,6-bisphosphate (F1,6BP), phosphoenolpyruvate (PEP), and 6-phosphogluconate (6PG) in T4V-ARO47m (Figure 4). Meanwhile, intermediates of the shikimate pathway [3-dehydroquinate (DHQ), 3-dehydroshikimate (DHS), shikimate, shikimate 3-phosphate (S3P), and chorismate] significantly accumulated in

the T4V-ARO47m strain which remained after complete glycerol consumption (96 h fermentation) (Figure 4). In addition, the accumulation of aromatic amino acids [L-Tyr, L-phenylalanine (L-Phe), and L-tryptophan (L-Trp)] was maintained at relatively high levels in this strain.

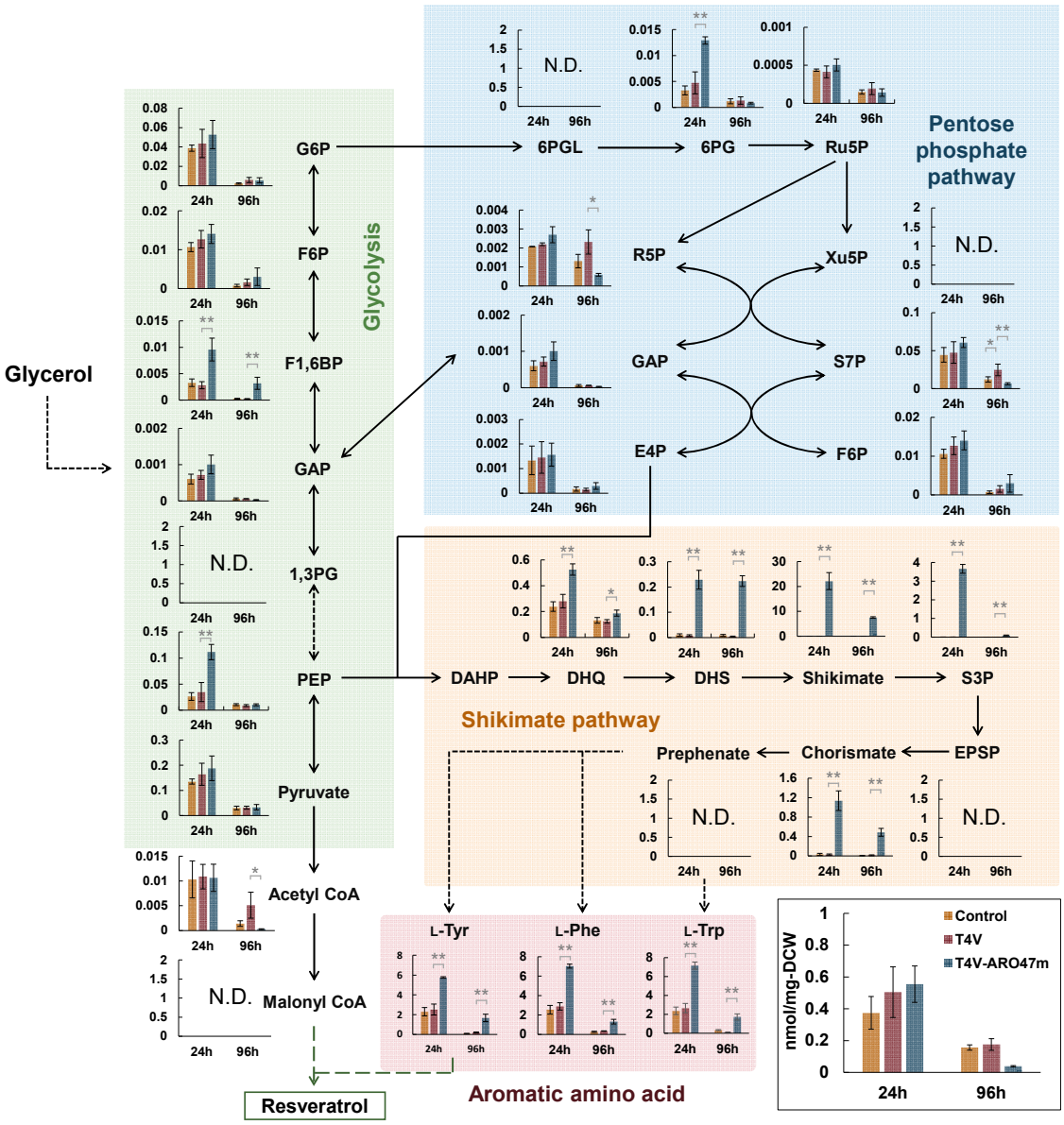

Figure 4. Comparison of intracellular metabolites involved in the resveratrol synthetic pathway in the T4V, T4V-ARO47m, and their parent strain. Intracellular metabolites were extracted after 24 and 96 h incubation in YPG medium. Metabolites

extracted from cells were subjected to LC-MS/MS analysis. T4V, T4V-ARO47m, and their parent strain CBS7435 *Δdnl4 Δhis4* (Control) were used for intracellular metabolite analysis. All y-axis units are in n-mol/mg-dry cell weight (DCW). The dashed arrows indicate multiple enzymatic steps. Error bars represent the standard deviations of three independent biological samples. Statistical analysis was performed using EZR (two-tailed, two-sample unequal variance; $*p < 0.05$, $**p < 0.005$). G6P; F6P; F1,6BP; GAP; 1,3PG; PEP; 6PGL; 6PG; Ru5P; R5P; Xu5P; S7P; E4P; DAHP3-deoxy-D-arabino; and EPSP as stated in Figure 1; DHQ: 3-dehydroquinate; DHS: 3-dehydroshikimate; S3P: shikimate 3-phosphate; L-Tyr: tyrosine; L-Phe: phenylalanine; L-Trp: tryptophan. N.D.: not detected.

Expanding the pathway to produce naringenin

A naringenin-producing strain (T4CC strain) was developed by introducing *HaTAL*, *At4CL*, chalcone synthase from *Hypericum androsaemum* (*HaCHS*), and chalcone isomerase from *Medicago sativa* (*MsCHI*) into the parent strain (*P. pastoris* CBS7435 *Δdnl4 Δhis4*). Furthermore, $ARO4^{K229L}$ and $ARO7^{G141S}$ were co-overexpressed in the T4CC strain (T4CC-ARO47m strain). The T4CC-ARO47m strain had a slight defect on cell growth (Supporting Figure S3) and produced 306 mg/L naringenin compared with 89 mg/L in the T4CC strain with a yield of 15.3 mg/g-glycerol consumed (Figure 5A). Fed-batch fermentation with controlled pH and DO in the T4CC-ARO47m strain produced 1067 mg/L naringenin with a yield of 9.7 mg/g-glycerol consumed after 120 h which was 249% higher than that in flasks (Figure 5B) and is the highest naringenin titer using a microbial host (Supporting Table S1).

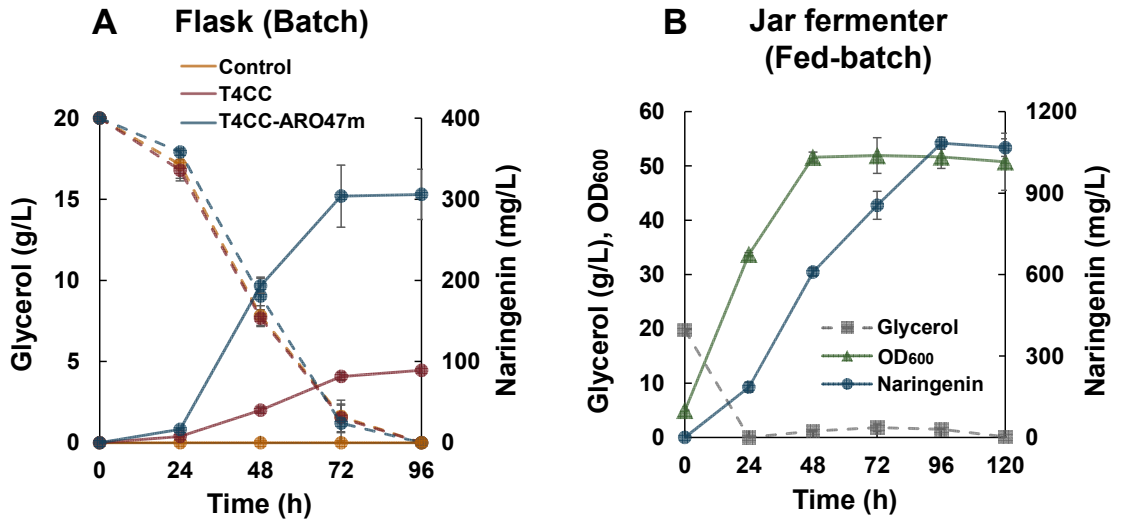

Figure 5. Naringenin production in the engineered *P. pastoris* strains. (A) Time course of naringenin production and glycerol consumption in YPG culture medium of naringenin-producing strains (T4CC and T4CC-ARO47m) and their parent strain CBS7435 *Δdnl4 Δhis4* (Control). Error bars represent standard deviations of three independent biological samples. The solid lines and dashed lines represent the naringenin titer and glycerol concentration, respectively. (B) Fed-batch fermentation results of the T4CC-ARO47m strain using the jar fermenter. The feed was added from 24 to 96 h. Error bars represent the standard deviations of two independent biological samples.

Production of BIAs in the engineered strains

A norcoclaurine-producing strain (CDN) was generated by introducing *BvCYP*$^{W13L, F309L}$, DOPA decarboxylase from *Pseudomonas putida* (*PpDODC*), and an N-terminal truncation of norcoclaurine synthase from *Coptis japonica* (*ΔN_CjNCS*), which increases norcoclaurine titer by 50% compared with full-length *CjNCS*[7]. *ARO4*^{K229L} and *ARO7*^{G141S} were co-overexpressed in the CDN strain to produce CDN-ARO47m. The CDN-ARO47m strain had a slight defect on cell growth

(Supporting Figure S4) and produced 10.6 mg/L norcoclaurine compared with 0.30 mg/L in the CDN strain (Figure 6A). Fed-batch fermentation with controlled pH and DO in the CDN-ARO47m produced 9.7 mg/L norcoclaurine which was comparable with batch conditions in flasks (Figure 6B).

Reticuline is the last shared intermediate in the major branch point of BIA production pathways and is produced from norcoclaurine via four enzymatic steps. Therefore, a reticuline-producing strain (CDN-ARO47m_6CN4 strain) was developed by introducing 6-*O*-methyltransferase (*Ps6OMT*), coclaurine *N*-methyltransferase (*PsCNMT*), and 4'-*O*-methyltransferase (*Ps4OMT*) from *Papaver somniferum*, and *N*-methylcoclaurine hydroxylase from *Eschscholzia californica* (*EcNMCH*) into the CDN-ARO47m strain. This strain produced reticuline at a titer of 292 µg/L (Figure 6C). This is the first report of the successful production of norcoclaurine and reticuline in *P. pastoris*.

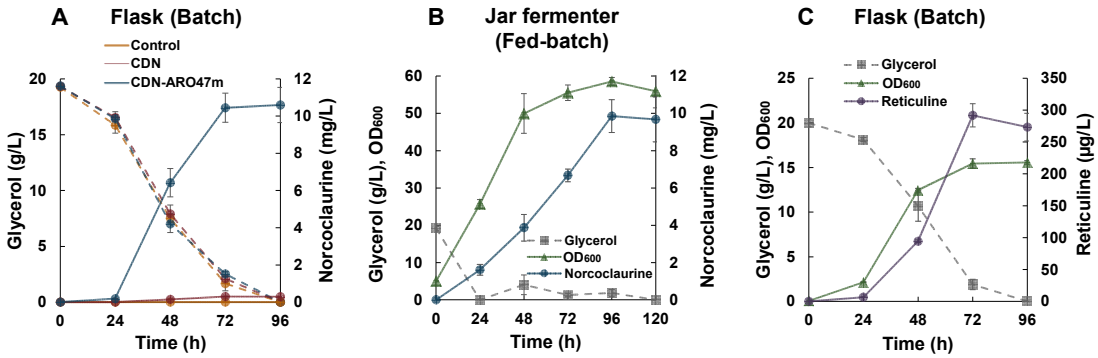

Figure 6. Production of BIAs (norcoclaurine and reticuline) in the engineered *P.pastoris* strains. (A) Time course of norcoclaurine production and glycerol consumption in YPG culture medium of norcoclaurine-producing strains (CDN and CDN-ARO47m) and their parent strain CBS7435 *Δdnl4 Δhis4* (Control). Error bars represent the standard deviation of three independent biological samples. The solid lines and dashed lines represent norcoclaurine titer and glycerol concentration, respectively. (B) Fed-batch fermentation results of CDN-ARO47m using the jar fermenter. The feed

was added from 24 to 96 h. Error bars represent the standard deviations of two independent biological samples. (C) Time course of reticuline production, glycerol consumption, and cell growth (OD_{600}) of CDN-ARO47m-6CN4. Error bars represent the standard deviations of three independent biological samples.

Production of various aromatic compounds from crude glycerol

One of the major challenges in microbial production is the high raw material cost. Resveratrol, naringenin, and norcoclaurine production were examined using crude glycerol by-product from BDF production. Neutralized crude glycerol containing 260.6 g/L glycerol and 54.6 g/L methanol was diluted to a glycerol concentration of 20 g/L and used as a carbon source for batch fermentation with T4V-ARO47m, T4CC-ARO47m, and CDN-ARO47m strains. T4V-ARO47m produced 383 mg/L resveratrol with a yield of 20.6 mg/g-crude glycerol consumed (Figure 7A), T4CC-ARO47m produced 338 mg/L naringenin with a yield of 18.4 mg/g-crude glycerol consumed (Figure 7B), and CDN-ARO47m produced 7.1 mg/L norcoclaurine with a yield of 0.34 mg/g-crude glycerol consumed (Figure 7C). In all fermentations, there was little difference in titer, cell growth, and glycerol consumption compared to cultivation with pure glycerol indicating that *P. pastoris* is capable of utilizing crude glycerol.

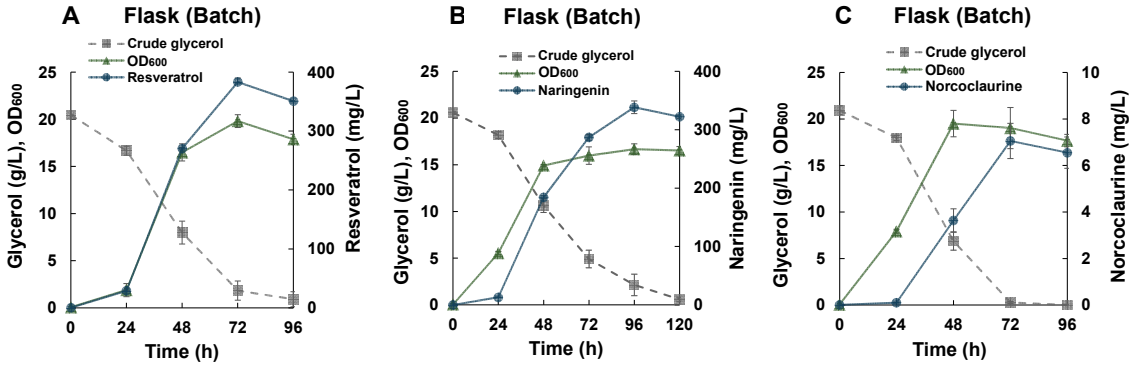

Figure 7. Aromatic compounds production from crude glycerol. (A) Resveratrol, (B)

naringenin, and (C) norcoclaurine production from crude glycerol as a carbon source in the T4V-ARO47m, T4CC-ARO47m, and CDN-ARO47m strains, respectively. Error bars represent the standard deviations of three independent biological samples.

DISCUSSION

Recent synthetic biology improvements indicate that *P. pastoris* is a promising platform for metabolic engineering and will likely become the next-generation yeast cell factory[21,24]. Optimization of the biosynthetic pathway for L-Tyr precursor is essential to achieve high production of various aromatic secondary metabolites[13,14] (Figure 1).

In this study, a fluorescence-based screening system was constructed by engineering *P. pastoris* to produce betaxanthin to identify the optimal genetic engineering strategies for high L-Tyr production from glycerol. Overexpression of $ARO4^{K229L}$ and $ARO7^{G141S}$ from *S. cerevisiae* enhanced L-Tyr titer in *P. pastoris* (Figure 2) with significant accumulation of the intracellular metabolites of the shikimate pathway (DHQ, DHS, shikimate, S3P, and chorismate) at the beginning of glycerol consumption (24 h) and at the end (96 h) (Figure 4). Meanwhile, overexpression of PPP genes *TKL1*, *SOL3*, and *ZWF1* had little positive effect on betaxanthin levels (Figure 2) which may be caused by the low activity of other PPP enzymes and/or the downstream shikimate pathway. In yeast, the five-step reaction from 3-deoxy-D-arabinoheptulosonate 7-phosphate (DAHP) to 5-*O*-(1-carboxyvinyl)-3-phosposhikimate (EPSP) in the shikimate pathway is catalyzed by ARO1p[29]. The *P. pastoris ARO1* overexpressing strain (T4V-ARO47m-ARO1) increased resveratrol titer by 15% to 544 mg/L (Supporting Figure S5A). However, *ARO1* overexpression resulted in significant defects in cell growth and glycerol consumption (Supporting Figure S5B, S5C) which may be caused by excessive flux to the shikimate pathway resulting in high intracellular toxicity. In other organisms such as

298 plants and bacteria, the five-steps DHAP to EPSP are catalyzed by monofunctional
299 enzymes. It has been reported that the overexpression of *E. coli* shikimate kinase AroL,
300 which catalyzes the conversion of shikimate to S3P, enhances the *p*-coumarate titer in *S.*
301 *cerevisiae*[30]. A similar engineering approach might improve the titer of L-Tyr-derived
302 compounds in *P. pastoris*.

303 Co-overexpression of $ARO4^{K229L}$ and $ARO7^{G141S}$ together with the *de novo*
304 pathways for the synthesis of resveratrol, naringenin, or norcoclaurine secondary
305 metabolites increased their titers by 258%, 344%, or 3400%, respectively compared
306 with the strains introduced only with the heterologous pathway (Figure 3A, 5A, 6A)
307 using glycerol as the carbon source. Resveratrol titer decreased by approximately half in
308 resveratrol-producing strains (T4V and T4V-ARO47m) cultured in YPD medium
309 containing 20 g/L glucose compared with glycerol: the T4V and T4V-ARO47m strain
310 produced 101 mg/L and 176 mg/L resveratrol, respectively using glucose (Supporting
311 Figure S6). Cell growth was comparable; however, glycerol was consumed over 96 h,
312 while glucose was consumed in 48 h (Supporting Figure S2, S6). A similar
313 phenomenon was reported for resveratrol production using glucose or sucrose carbon
314 sources in *Scheffersomyces stipitis* engineered to synthesize resveratrol: 237.6 mg/L
315 resveratrol was produced with 50 g/L glucose consumed in 24 h or 668.6 mg/L
316 resveratrol was produced and 50 g/L sucrose consumed over 96 h[28]. These results
317 suggest that the rate of carbon uptake may affect resveratrol production. Further studies
318 will be needed to elucidate the detailed metabolic mechanisms and physiology of *P.*
319 *pastoris* by examining differences in intracellular metabolites and protein expression
320 levels when cultured with glucose or glycerol.

321 In fed-batch fermentation, the resveratrol, naringenin, and norcoclaurine titer
322 reached 1825 mg/L and 1067 mg/L, and 9.7 mg/L, respectively (Figure 3B, 5B, 6B).
323 There was little difference in norcoclaurine titer between batch and fed-batch
324 fermentation (Figure 6A, 6B). The cytoplasmic expression of norcoclaurine synthase

(*NCS*) is toxic to *S. cerevisiae* resulting in reduced norcoclaurine and reticuline production[31]. Toxicity was reduced and reticuline titer increased by the addition of a peptide tag to the C-terminus (peroxisomal targeting signal type 1, PTS1) of NCS to compartmentalize NCS into peroxisomes[31]. This approach may be useful for *P. pastoris.* For better understanding toxicity and productivity of L-Tyr-derived compounds, it will be important to examine their intracellular accumulation.

Crude glycerol by-product from BDF production contains impurities such as free fatty acids, inorganic salts, and methanol[32,33] and its purification require sequential treatments including neutralization, distillation, ion exchange, membrane separation, and activated carbon adsorption[34]. Distillation and ion exchange are energy- and cost-intensive processes and the total purification cost for commercial production is up to $50.45/kg[34,35]. This cost is much higher than the current market price of pure glycerol ($1-15/kg)[36] resulting in crude glycerol disposal. Thus, conversion of crude glycerol into value-added products generates economic and environmental benefits[32,36]. In the present study, resveratrol, naringenin, and norcoclaurine were synthesized using neutralized crude glycerol to the same levels as that with pure glycerol (Figure 7). This is the first report of L-Tyr-derived aromatic compound production from crude glycerol which demonstrates the potential of *P. pastoris* to utilize crude glycerol for the synthesis of various aromatic compounds.

In this study, an L-Tyr chassis was produced to optimize L-Tyr synthesis from glycerol in *P. pastoris*. A heterologous pathway was introduced into the engineered strain for the *de novo* production of various L-Tyr-derived aromatic compounds. A major improvement in the production of aromatic secondary metabolites resveratrol, naringenin, norcoclaurine, and reticuline was observed. This study will accelerate the development of *P. pastoris* strains capable of producing high value aromatic compounds from glycerol.

METHODS

Strains and media conditions

Escherichia coli NovaBlue (Merck Millipore, Darmstadt, Germany) was used for plasmid construction and amplification. The microorganisms were routinely cultured at 37 °C and 200 rpm in LB medium [10 g/L tryptone (Nacalai Tesque, Kyoto, Japan), 5 g/L yeast extract (Nacalai Tesque), and 5 g/L NaCl] supplemented with 100 μg/mL ampicillin.

The yeast strains used in this study are listed in Table 1. *P. pastoris* CBS7435 *Δdnl4 Δhis4* was used as a parent strain since it has improved gene targeting efficiency for homologous recombination[37]. *P. pastoris* strains were cultivated in YPG medium [10 g/L yeast extract, 20 g/L peptone (BD Biosciences, San Jose, CA, USA), and 20 g/L glycerol], YPD medium [10 g/L yeast extract, 20 g/L peptone, and 20 g/L glucose], or SD medium [6.7 g/L yeast nitrogen base without amino acids (Difco Laboratories, Detroit, MI, USA), and 20 g/L glucose] supplemented with 20 mg/L histidine and appropriate antibiotics including 500 μg/mL G418 (FUJIFILM Wako Pure Chemical, Osaka, Japan), 300 μg/mL hygromycin (Nacalai Tesque), 100 μg/mL Zeocin (Nacalai Tesque), and 50 μg/mL clonNAT (Jena Bioscience, Löbstedter, Germany).

Plasmid construction and yeast strains

Plasmids, synthetic DNA fragments, and primers are listed in Table 1, Supporting Table S2, and Table S3, respectively. Synthetic DNA fragments of *HaTAL*, *At4CL*, and *VvVST* were used as previously reported[28]. All other synthetic DNA fragments were codon-optimized for *P. pastoris* and synthesized by GeneArt (Thermo Fisher Scientific, Waltham, MA, USA). All plasmids were constructed using the In-fusion HD cloning kit (Takara Bio USA, Mountain View, CA, USA) according to the manufacturer's protocol. Detailed methods for plasmid and strain construction are provided in the supporting information.

Batch fermentation

Yeast cells were inoculated into 5 mL of YPG medium supplemented with appropriate antibiotics in test tubes and pre-cultured overnight at 30 °C and 200 rpm. Cells were centrifuged at 15,000 × *g* for 1 min, washed twice with sterile water, inoculated in 20 mL YPG medium in 100-mL Erlenmeyer flasks with a cap-type plug at an initial OD_{600} of 0.05, and cultivated at 30 °C and 150 rpm in an orbital shaker incubator (BR-43FL; Taitec, Saitama, Japan). The culture broth was used to measure OD_{600} and the concentration of glucose, glycerol, resveratrol, naringenin, norcoclaurine, reticuline, and intracellular metabolites was measured as described below.

Fluorescence-based screening with betaxanthin

Yeast cells were centrifuged at 15,000 × *g* for 1 min after 24 h cultivation in YPG medium as described above. Two hundred and fifty μL of culture supernatant was transferred to a 96-well black plate (Sumitomo Bakelite, Tokyo, Japan) and fluorescence intensity was measured using an excitation wavelength of 485 nm and emission wavelength of 510 nm to determine betaxanthin levels using Envision 2014 multilabel plate reader (PerkinElmer, Waltham, MA, USA).

Fed-batch fermentation in jar fermenter

Yeast cells were pre-cultured in 20 mL of YPG medium supplemented with appropriate antibiotics in a 100-mL Erlenmeyer flask at 30 °C and 150 rpm for 48 h. Cells in stationary phase were centrifuged at 5,000 × *g* for 5 min, washed twice with sterile water, suspended in 100 mL YPG medium and transferred into a 250-mL jar fermenter (Bio Jr. 8; ABLE Biott, Tokyo, Japan) at an initial OD_{600} of 5.0. Fermentation was carried out at 30 °C and the airflow was maintained at 100 mL/min. The pH of the culture medium was maintained at 5.5 by the automatic addition of a 5 N ammonium

406 solution, and antifoam SI (FUJIFILM Wako Pure Chemical, Osaka, Japan) was added in
407 the range of 0.01-0.1 %. The agitation speed varied between 300 and 600 rpm to
408 maintain dissolved oxygen (DO) at 20%. A feeding solution composed of 50 g/L yeast
409 extract, 100 g/L peptone, and 200 g/L glycerol was pumped into the jar fermenter at a
410 flow rate of 625 μL/h (45 mL total volume) after 24 h fermentation. Approximately 1
411 mL samples were withdrawn every 24 h to measure OD_{600} and the concentration of
412 glycerol, resveratrol, naringenin, and norcoclaurine.
413
414 **Purification of crude glycerol**
415 Crude glycerol, a major by-product from the biodiesel industry, was kindly
416 provided by the Sannokura Center (Gifu, Japan) and pretreated according to the method
417 described by Chi et al[38]. Briefly, the pH of crude glycerol was adjusted to 6.3 with 1 N
418 HCl, stirred for 2 h at room temperature, added to a separatory funnel, and the lower
419 layer collected and filtered through a 0.22 μm filter. The glycerol and methanol
420 concentrations in the filtered liquid was analyzed as described below. The filtered liquid
421 was diluted with sterile water to a final glycerol concentration of 20 g/L together with
422 10 g/L yeast extract and 20 g/L peptone in the culture medium. Batch fermentation was
423 performed using the same conditions as described above.
424
425 **Analytical methods**
426 The concentrations of glucose, glycerol, and methanol were analyzed by
427 high-performance liquid chromatography (HPLC) (Shimadzu, Kyoto, Japan) equipped
428 with an Aminex HPX-87H column (7.8 mm × 300 mm, 9 μm particle size; Bio-Rad,
429 Hercules, CA, USA) and a RID-10A refractive index detector (Shimadzu). The column
430 was kept at 65 °C, and 5 mM H_2SO_4 was used as the mobile phase at a flow rate of 0.6
431 mL/min. For resveratrol and naringenin quantification, culture samples were mixed with
432 an equal volume of 100% ethanol, vortexed for 10 s, and centrifugated at 15,000 × *g* for

5 min at room temperature[28,39]. These supernatants were then analyzed by HPLC equipped with a Luna Omega PS C18 column (4.6 × 150 mm, 3 μm particle size; Phenomenex, CA, USA) as described previously[28]. Quantification of norcoclaurine and reticuline in the fermentation medium was carried out with an LCMS-8060 triple quadrupole mass spectrometer (Shimadzu) equipped with a Discovery HS F5-3 column (2.1 mm × 150 mm, 3 μm, Sigma-Aldrich, MO, USA) using previously described running conditions[40].

Intracellular metabolite analysis

The extraction method for intracellular metabolites followed a previously described method[41]. Intracellular metabolites related to amino acids and the shikimate pathway were analyzed using the LCMS-8060 instrument described above. Metabolites related to glycolysis and PPP were analyzed using a 6460 Triple Quad LC/MS (Agilent Technologies, CA, USA) equipped with a Mastro C18 column (2.1 mm × 150 mm, 3 μm, Shimadzu) using previously described running conditions[40,42].

Statistical analysis

All numerical values are depicted as the means ± s.d. One-way ANOVA was used as a statistical test in conjunction with Tukey's range test to assess significant differences between strains. Statistical analysis was performed using EZR[43] which is a modified version of R commander designed to add frequently used statistical functions in biostatistics (two-tailed, two-sample unequal variance; $*p < 0.05$, $**p < 0.005$).

Table 1 Yeast strains and plasmids

Strains	Description	Source
CBS7435 *Δdnl4 Δhis4*	Δdnl4 Δhis4 :: ADE1	[37]
CD	CBS7435 *Δdnl4 Δhis4* / pPGP-CYP-DOD [$G418^r$]	This study
CD-TKL1	CD / pPGPZ-TKL1 [$G418^r$, Zeo^r]	This study

CD-SOL3	CD / pPGPZ-SOL3 [G418^r, Zeo^r]	This study
CD-ZWF1	CD / pPGPZ-ZWF1 [G418^r, Zeo^r]	This study
CD-SOL3-ZWF1	CD / pPGPZ-SOL3-ZWF1 [G418^r, Zeo^r]	This study
CD-ARO4m	CD / pPGPH-ARO4^{K229L} [G418^r, Hyg^r]	This study
CD-ARO7m	CD / pPGPZ-ARO7^{G141S} [G418^r, Zeo^r]	This study
CD47m	CD / pPGPH-ARO4^{K229L}-ARO7^{G141S} [G418^r, Hyg^r]	This study
CD47m-TKL1	CD47m / pPGPZ-TKL1 [G418^r, Zeo^r, Hyg^r]	This study
CD47m-SOL3	CD47m / pPGPZ-SOL3 [G418^r, Zeo^r, Hyg^r]	This study
CD47m-ZWF1	CD47m / pPGPZ-ZWF1 [G418^r, Zeo^r, Hyg^r]	This study
CD47m-SOL3-ZWF1	CD47m / pPGPZ-SOL3-ZWF1 [G418^r, Zeo^r, Hyg^r]	This study
T4V	CBS7435 *Δdnl4 Δhis4* / pPGP-TAL-4CL-VST [G418^r]	This study
T4V-ARO47m	T4V / pPGPH-ARO4^{K229L}-ARO7^{G141S} [G418^r, Hyg^r]	This study
T4CC	CBS7435 *Δdnl4 Δhis4* / pPGP-TAL-4CL, pPGPZ-CHS-CHI [G418^r, Zeo^r]	This study
T4CC-ARO47m	T4CC / pPGPH-ARO4^{K229L}-ARO7^{G141S} [G418^r, Zeo^r, Hyg^r]	This study
CDN	CBS7435 *Δdnl4 Δhis4* / pPGP-CYP-DODC, pPGPZ-NCS [G418^r, Zeo^r]	This study
CDN-ARO47m	CDN / pPGPH-ARO4^{K229L}-ARO7^{G141S} [G418^r, Zeo^r, Hyg^r]	This study
CDN-ARO47m-6CN4	CDN-ARO47m / pPHU-6OMT-CNMT, pPNS-NMCH-4OMT [G418^r, Zeo^r, Hyg^r, NAT^r, *his4*]	This study
Plasmids		
pPGP-EGFP	G418^r, P_{gap}-*EGFP*-T_{aox1}	[37]
pPGP-CYP	G418^r, P_{gap}-*BvCYP*$^{W13L, F309L}$-T_{aox1}	[44]
pPGPH-DOD	Hyg^r, P_{gap}-*MjDOD*-T_{aox1}	[44]
pPGPZ-EGFP	Zeo^r, P_{gap}-*EGFP*-T_{aox1}	This study
pPGP-CYP-DOD	G418^r, P_{gap}-*BvCYP*$^{W13L, F309L}$-T_{aox1},	This study

	P_{gap}-*MjDOD*-T_{aox1}	
pPGPZ-TKL1	Zeo^r, P_{gap}-*TKL1*-T_{aox1}	This study
pPGPZ-SOL3	Zeo^r, P_{gap}-*SOL3*-T_{aox1}	This study
pPGPZ-ZWF1	Zeo^r, P_{gap}-*ZWF1*-T_{aox1}	This study
pPGPZ-SOL3-ZWF1	Zeo^r, P_{gap}-*SOL3*-T_{aox1}, P_{gap}-*ZWF1*-T_{aox1}	This study
pPGPH-ARO4^{K229L}	Hyg^r, P_{gap}-*ARO4*^{K229L}-T_{aox1}	This study
pPGPZ-ARO7^{G141S}	Zeo^r, P_{gap}-*ARO7*^{G141S}-T_{aox1}	This study
pPGPH-ARO4^{K229L}-ARO7^{G141S}	Hyg^r, P_{gap}-*ARO4*^{K229L} -T_{aox1}, P_{gap}-*ARO7*^{G141S}-T_{aox1}	This study
pPGPZ-ARO1	Zeo^r, P_{gap}-*ARO1*-T_{aox1}	This study
pPGP-TAL	G418^r, P_{gap}-*HaTAL*-T_{aox1},	This study
pPGP-4CL	G418^r, P_{gap}-*At4CL*-T_{aox1},	This study
pPGPZ-VST	Zeo^r, P_{gap}-*VvVST*-T_{aox1}	This study
pPGP-TAL-VST	G418^r, P_{gap}-*HaTAL*-T_{aox1}, P_{gap}-*VvVST*-T_{aox1}	This study
pPGP-TAL-4CL-VST	G418^r, P_{gap}-*HaTAL*-T_{aox1}, P_{gap}-*At4CL*-T_{aox1}	This study
	P_{gap}-*VvVST*-T_{aox1},	
pPGP-TAL-4CL	G418^r, P_{gap}-*HaTAL*-T_{aox1}, P_{gap}-*At4CL*-T_{aox1}	This study
pPGPZ-CHS	Zeo^r, P_{gap}-*HaCHS*-T_{aox1}	This study
pPGPZ-CHI	Zeo^r, P_{gap}-*MsCHI*-T_{aox1}	This study
pPGPZ-CHS-CHI	Zeo^r, P_{gap}-*HaCHS*-T_{aox1}, P_{gap}-*MsCHI*-T_{aox1}	This study
pPHU	*HIS4* marker,	This study
pPNS	NAT^r	This study
pPGPZ-DODC	Zeo^r, P_{gap}-*PpDODC*-T_{aox1}	This study
pPGP-CYP-DODC	G418^r, P_{gap}-*BvCYP*$^{W13L, F309L}$-T_{aox1},	This study
	P_{gap}-*PpDODC*-T_{aox1}	
pPGPZ-NCS	Zeo^r, P_{gap}-*ΔN_CjNCS*-T_{aox1}	This study
pPGPZ-6OMT	Zeo^r, P_{gap}-*Ps6OMT*-T_{aox1}	This study
pPGPZ-CNMT	Zeo^r, P_{gap}-*PsCNMT*-T_{aox1}	This study
pPGPZ-NMCH	Zeo^r, P_{gap}-*EcNMCH*-T_{aox1}	This study
pPGPZ-4OMT	Zeo^r, P_{gap}-*Ps4OMT*-T_{aox1}	This study
pPHU-6OMT	*HIS4* marker, P_{gap}-*Ps6OMT*-T_{aox1}	This study
pPHU-6OMT-CNMT	*HIS4* marker, P_{gap}-*Ps6OMT*-T_{aox1},	This study

	P_{gap}-*PsCNMT*-T_{aox1}	
pPNS-NMCH	NAT^r, P_{gap}-*EcNMCH*-T_{aox1}	This study
pPNS-NMCH-4OMT	NAT^r, P_{gap}-*EcNMCH*-T_{aox1}, P_{gap}-*Ps4OMT*-T_{aox1}	This study

ASSOCIATED CONTENT

Supporting Information

Detailed methods for plasmid and yeast strain construction; Supporting Figure S1, Difference in yeast colony coloration and green fluorescence for betaxanthin-producing cells; Supporting Figure S2-S4, Cell growth of engineered strains; Supporting Figure S5, The data of resveratrol production in ARO1 overexpressing strain; Supporting Figure S6, The data of resveratrol production using glucose; Supporting Table S1, Comparison of resveratrol, naringenin, norcoclaurine, and reticuline titer by various microbial hosts; Supporting Table S2, Synthetic DNA fragments; Supporting Table S3, Primer list.

AUTHOR INFORMATION

Corresponding Author

Tomohisa Hasunuma —Engineering Biology Research Center, Kobe University, 1-1 Rokkodai, Nada, Kobe, 657-8501, Japan; orcid.org/0000-0002-8382-2362; Phone: +81-78-803-6461;

E-mail: hasunuma@port.kobe-u.ac.jp; Fax: +81-78-803-6461

Authors

Ryota KUMOKITA — Graduate School of Science, Technology and Innovation, Kobe University, 1-1 Rokkodai, Nada, Kobe 657-8501, Japan

Takahiro Bamba — Graduate School of Science, Technology and Innovation, Kobe University, 1-1 Rokkodai, Nada, Kobe 657-8501, Japan

Kentaro Inokuma — Graduate School of Science, Technology and Innovation, Kobe University, 1-1 Rokkodai, Nada, Kobe 657-8501, Japan

Takanobu Yoshida — Graduate School of Science, Technology and Innovation, Kobe University, 1-1 Rokkodai, Nada, Kobe 657-8501, Japan

Yoichiro Ito — Graduate School of Science, Technology and Innovation, Kobe University, 1-1 Rokkodai, Nada, Kobe 657-8501, Japan

Akihiko Kondo — Graduate School of Science, Technology and Innovation, Kobe University, 1-1 Rokkodai, Nada, Kobe 657-8501, Japan

Authorship Contributions

R. K. and T. B. conceived the topic and designed the study. R. K. performed all genetic engineering and fermentation experiments. T. Y. analyzed the data. All authors discussed the results. R. K. wrote the manuscript supported from T.B., K. I., and T. H. Y. I., A. K., and T. H. supervised all aspects of the study.

Notes

The authors declare no conflict of interest.

ACKNOWLEDGEMENTS

The authors are grateful for support from the NEDO project P16009 (Development of production techniques for highly functional biomaterials using plant and other organism smart cells) and P20011 (Development of bio-derived product production technology that accelerates the realization of carbon recycling).

505

506 **REFERENCES**

507 (1) Newman, D. J.; Cragg, G. M. Natural Products as Sources of New Drugs from
508 1981 to 2014. *J. Nat. Prod.* **2016**, *79* (3), 629–661.
509 https://doi.org/10.1021/acs.jnatprod.5b01055.

510 (2) Navarro, G.; Martínez Pinilla, E.; Ortiz, R.; Noé, V.; Ciudad, C. J.; Franco, R.
511 Resveratrol and Related Stilbenoids, Nutraceutical/Dietary Complements with
512 Health-Promoting Actions: Industrial Production, Safety, and the Search for
513 Mode of Action. *Compr. Rev. Food Sci. Food Saf.* **2018**, *17* (4), 808–826.
514 https://doi.org/10.1111/1541-4337.12359.

515 (3) Milke, L.; Aschenbrenner, J.; Marienhagen, J.; Kallscheuer, N. Production of
516 Plant-Derived Polyphenols in Microorganisms: Current State and Perspectives.
517 *Appl. Microbiol. Biotechnol.* **2018**, *102* (4), 1575–1585.
518 https://doi.org/10.1007/s00253-018-8747-5.

519 (4) Facchini, P. J.; Bohlmann, J.; Covello, P. S.; Luca, V. De; Mahadevan, R.; Page,
520 J. E.; Ro, D.; Sensen, C. W.; Storms, R.; Martin, V. J. J. Synthetic Biosystems for
521 the Production of High-Value Plant Metabolites. *Trends Biotechnol.* **2012**, *30* (3),
522 127–131. https://doi.org/10.1016/j.tibtech.2011.10.001.

523 (5) Glenn, W. S.; Runguphan, W.; Connor, S. E. O. Recent Progress in the Metabolic
524 Engineering of Alkaloids in Plant Systems. *Curr. Opin. Biotechnol.* **2013**, *24* (2),
525 354–365. https://doi.org/10.1016/j.copbio.2012.08.003.

526 (6) Pyne, M. E.; Narcross, L.; Martin, V. J. J. Engineering Plant Secondary
527 Metabolism in Microbial Systems. *Plant Physiol.* **2019**, *179* (3), 844–861.
528 https://doi.org/10.1104/pp.18.01291.

529 (7) Pyne, M. E.; Kevvai, K.; Grewal, P. S.; Narcross, L.; Choi, B.; Bourgeois, L.;
530 Dueber, J. E.; Martin, V. J. J. A Yeast Platform for High-Level Synthesis of
531 Tetrahydroisoquinoline Alkaloids. *Nat. Commun.* **2020**, *11* (1), 1–10.

https://doi.org/10.1038/s41467-020-17172-x.

(8) Zhou, S.; Hao, T.; Zhou, J. Fermentation and Metabolic Pathway Optimization to de Novo Synthesize (2S)-Naringenin in Escherichia Coli. *J. Microbiol. Biotechnol.* **2020**, *30* (10), 1574–1582. https://doi.org/10.4014/JMB.2008.08005.

(9) Cravens, A.; Payne, J.; Smolke, C. D. Synthetic Biology Strategies for Microbial Biosynthesis of Plant Natural Products. *Nat. Commun.* **2019**, *10* (1), 1–12. https://doi.org/10.1038/s41467-019-09848-w.

(10) Yuan, S. F.; Alper, H. S. Metabolic Engineering of Microbial Cell Factories for Production of Nutraceuticals. *Microb. Cell Fact.* **2019**, *18* (1), 1–11. https://doi.org/10.1186/s12934-019-1096-y.

(11) Suástegui, M.; Shao, Z. Yeast Factories for the Production of Aromatic Compounds: From Building Blocks to Plant Secondary Metabolites. *J. Ind. Microbiol. Biotechnol.* **2016**, *43* (11), 1611–1624. https://doi.org/10.1007/s10295-016-1824-9.

(12) Gottardi, M.; Reifenrath, M.; Boles, E.; Tripp, J. Pathway Engineering for the Production of Heterologous Aromatic Chemicals and Their Derivatives in Saccharomyces Cerevisiae: Bioconversion from Glucose. *FEMS Yeast Res.* **2017**, *17* (4), 1–11. https://doi.org/10.1093/femsyr/fox035.

(13) Liu, Q.; Liu, Y.; Chen, Y.; Nielsen, J. Current State of Aromatics Production Using Yeast: Achievements and Challenges. *Curr. Opin. Biotechnol.* **2020**, *65*, 65–74. https://doi.org/10.1016/j.copbio.2020.01.008.

(14) Rajkumar, A. S.; Morrissey, J. P. Rational Engineering of Kluyveromyces Marxianus to Create a Chassis for the Production of Aromatic Products. *Microb. Cell Fact.* **2020**, *19* (1), 1–19. https://doi.org/10.1186/s12934-020-01461-7.

(15) Krivoruchko, A.; Nielsen, J. Production of Natural Products through Metabolic Engineering of Saccharomyces Cerevisiae. *Curr. Opin. Biotechnol.* **2015**, *35*, 7–15. https://doi.org/10.1016/j.copbio.2014.12.004.

559 (16) Narcross, L.; Fossati, E.; Bourgeois, L.; Dueber, J. E.; Martin, V. J. J. Microbial
560 Factories for the Production of Benzylisoquinoline Alkaloids. *Trends Biotechnol.*
561 **2016**, *34* (3), 228–241. https://doi.org/10.1016/j.tibtech.2015.12.005.
562 (17) Li, Y.; Mao, J.; Liu, Q.; Song, X.; Wu, Y.; Cai, M.; Xu, H.; Qiao, M. De Novo
563 Biosynthesis of Caffeic Acid from Glucose by Engineered Saccharomyces
564 Cerevisiae. *ACS Synth. Biol.* **2020**, *9* (4), 756–765.
565 https://doi.org/10.1021/acssynbio.9b00431.
566 (18) Patra, P.; Das, M.; Kundu, P.; Ghosh, A. Recent Advances in Systems and
567 Synthetic Biology Approaches for Developing Novel Cell-Factories in
568 Non-Conventional Yeasts. *Biotechnol. Adv.* **2021**, *47* (December 2020), 107695.
569 https://doi.org/10.1016/j.biotechadv.2021.107695.
570 (19) Palmer, C. M.; Miller, K. K.; Nguyen, A.; Alper, H. S. Engineering
571 4-Coumaroyl-CoA Derived Polyketide Production in Yarrowia Lipolytica
572 through a β-Oxidation Mediated Strategy. *Metab. Eng.* **2020**, *57* (November
573 2019), 174–181. https://doi.org/10.1016/j.ymben.2019.11.006.
574 (20) Sáez-Sáez, J.; Wang, G.; Marella, E. R.; Sudarsan, S.; Cernuda Pastor, M.;
575 Borodina, I. Engineering the Oleaginous Yeast Yarrowia Lipolytica for
576 High-Level Resveratrol Production. *Metab. Eng.* **2020**, *62* (April), 51–61.
577 https://doi.org/10.1016/j.ymben.2020.08.009.
578 (21) Yang, Z.; Zhang, Z. Engineering Strategies for Enhanced Production of Protein
579 and Bio-Products in Pichia Pastoris: A Review. *Biotechnol. Adv.* **2018**, *36* (1),
580 182–195. https://doi.org/10.1016/j.biotechadv.2017.11.002.
581 (22) Wen, J.; Tian, L.; Liu, Q.; Zhang, Y.; Cai, M. Engineered Dynamic Distribution
582 of Malonyl-CoA Flux for Improving Polyketide Biosynthesis in Komagataella
583 Phaffii. *J. Biotechnol.* **2020**, *320* (April), 80–85.
584 https://doi.org/10.1016/j.jbiotec.2020.06.012.
585 (23) Hagman, A.; Säll, T.; Piškur, J. Analysis of the Yeast Short-Term Crabtree Effect

586 and Its Origin. *FEBS J.* **2014**, *281* (21), 4805–4814.
587 https://doi.org/10.1111/febs.13019.
588 (24) Peña, D. A.; Gasser, B.; Zanghellini, J.; Steiger, M. G.; Mattanovich, D.
589 Metabolic Engineering of Pichia Pastoris. *Metab. Eng.* **2018**, *50* (February), 2–15.
590 https://doi.org/10.1016/j.ymben.2018.04.017.
591 (25) Mattanovich, D.; Graf, A.; Stadlmann, J.; Dragosits, M.; Redl, A.; Maurer, M.;
592 Kleinheinz, M.; Sauer, M.; Altmann, F.; Gasser, B. Genome, Secretome and
593 Glucose Transport Highlight Unique Features of the Protein Production Host
594 Pichia Pastoris. *Microb. Cell Fact.* **2009**, *8*, 1–13.
595 https://doi.org/10.1186/1475-2859-8-29.
596 (26) Palmerín-Carreño, D.; Martínez-Alarcón, D.; Dena-Beltrán, J. L.; Vega-Rojas, L.
597 J.; Blanco-Labra, A.; Escobedo-Reyes, A.; García-Gasca, T. Optimization of a
598 Recombinant Lectin Production in Pichia Pastoris Using Crude Glycerol in a
599 Fed-Batch System. *Processes* **2021**, *9* (5). https://doi.org/10.3390/pr9050876.
600 (27) Nocon, J.; Steiger, M.; Mairinger, T.; Hohlweg, J.; Rußmayer, H.; Hann, S.;
601 Gasser, B.; Mattanovich, D. Increasing Pentose Phosphate Pathway Flux
602 Enhances Recombinant Protein Production in Pichia Pastoris. *Appl. Microbiol.*
603 *Biotechnol.* **2016**, *100* (13), 5955–5963.
604 https://doi.org/10.1007/s00253-016-7363-5.
605 (28) Kobayashi, Y.; Inokuma, K.; Matsuda, M.; Kondo, A.; Hasunuma, T. Resveratrol
606 Production from Several Types of Saccharide Sources by a Recombinant
607 Scheffersomyces Stipitis Strain. *Metab. Eng. Commun.* **2021**, *13* (October),
608 e00188. https://doi.org/10.1016/j.mec.2021.e00188.
609 (29) Liu, Q.; Yu, T.; Li, X.; Chen, Y.; Campbell, K.; Nielsen, J.; Chen, Y. Rewiring
610 Carbon Metabolism in Yeast for High Level Production of Aromatic Chemicals.
611 *Nat. Commun.* **2019**, *10* (1), 1–13. https://doi.org/10.1038/s41467-019-12961-5.
612 (30) Rodriguez, A.; Kildegaard, K. R.; Li, M.; Borodina, I.; Nielsen, J. Establishment

of a Yeast Platform Strain for Production of P-Coumaric Acid through Metabolic Engineering of Aromatic Amino Acid Biosynthesis. *Metab. Eng.* **2015**, *31*, 181-188. https://doi.org/10.1016/j.ymben.2015.08.003.

(31) Grewal, P. S.; Samson, J. A.; Baker, J. J.; Choi, B.; Dueber, J. E. Peroxisome Compartmentalization of a Toxic Enzyme Improves Alkaloid Production. *Nat. Chem. Biol.* **2021**, *17* (1), 96–103. https://doi.org/10.1038/s41589-020-00668-4.

(32) Luo, Z.; Miao, J.; Luo, W.; Li, G.; Du, Y.; Yu, X. Crude Glycerol from Biodiesel as a Carbon Source for Production of a Recombinant Highly Thermostable β-Mannanase by Pichia Pastoris. *Biotechnol. Lett.* **2018**, *40* (1), 135–141. https://doi.org/10.1007/s10529-017-2451-x.

(33) Do, D. T. H.; Theron, C. W.; Fickers, P. Organic Wastes as Feedstocks for Non-Conventional Yeast-Based Bioprocesses. *Microorganisms* **2019**, *7* (8), 1–22. https://doi.org/10.3390/microorganisms7080229.

(34) Ardi, M. S.; Aroua, M. K.; Hashim, N. A. Progress, Prospect and Challenges in Glycerol Purification Process: A Review. *Renew. Sustain. Energy Rev.* **2015**, *42*, 1164–1173. https://doi.org/10.1016/j.rser.2014.10.091.

(35) Chol, C. G.; Dhabhai, R.; Dalai, A. K.; Reaney, M. Purification of Crude Glycerol Derived from Biodiesel Production Process: Experimental Studies and Techno-Economic Analyses. *Fuel Process. Technol.* **2018**, *178* (May), 78–87. https://doi.org/10.1016/j.fuproc.2018.05.023.

(36) Kumar, L. R.; Kaur, R.; Tyagi, R. D.; Drogui, P. Identifying Economical Route for Crude Glycerol Valorization: Biodiesel versus Polyhydroxy-Butyrate (PHB). *Bioresour. Technol.* **2021**, *323* (December 2020), 124565. https://doi.org/10.1016/j.biortech.2020.124565.

(37) Ito, Y.; Watanabe, T.; Aikawa, S.; Nishi, T.; Nishiyama, T.; Nakamura, Y.; Hasunuma, T.; Okubo, Y.; Ishii, J.; Kondo, A. Deletion of DNA Ligase IV Homolog Confers Higher Gene Targeting Efficiency on Homologous

Recombination in Komagataella Phaffii. *FEMS Yeast Res.* **2018**, *18* (7), 1–9. https://doi.org/10.1093/femsyr/foy074.

(38) Chi, Z.; Pyle, D.; Wen, Z.; Frear, C.; Chen, S. A Laboratory Study of Producing Docosahexaenoic Acid from Biodiesel-Waste Glycerol by Microalgal Fermentation. *Process Biochem.* **2007**, *42* (11), 1537–1545. https://doi.org/10.1016/j.procbio.2007.08.008.

(39) Li, M.; Schneider, K.; Kristensen, M.; Borodina, I.; Nielsen, J. Engineering Yeast for High-Level Production of Stilbenoid Antioxidants. *Sci. Rep.* **2016**, *6*, 1–8. https://doi.org/10.1038/srep36827.

(40) Vavricka, C. J.; Yoshida, T.; Kuriya, Y.; Takahashi, S.; Ogawa, T.; Ono, F.; Agari, K.; Kiyota, H.; Li, J.; Ishii, J.; Tsuge, K.; Minami, H.; Araki, M.; Hasunuma, T.; Kondo, A. Mechanism-Based Tuning of Insect 3,4-Dihydroxyphenylacetaldehyde Synthase for Synthetic Bioproduction of Benzylisoquinoline Alkaloids. *Nat. Commun.* **2019**, *10* (1), 1–11. https://doi.org/10.1038/s41467-019-09610-2.

(41) Kato, H.; Izumi, Y.; Hasunuma, T.; Matsuda, F.; Kondo, A. Widely Targeted Metabolic Profiling Analysis of Yeast Central Metabolites. *J. Biosci. Bioeng.* **2012**, *113* (5), 665–673. https://doi.org/10.1016/j.jbiosc.2011.12.013.

(42) Hsu, H. H.; Araki, M.; Mochizuki, M.; Hori, Y.; Murata, M.; Kahar, P.; Yoshida, T.; Hasunuma, T.; Kondo, A. A Systematic Approach to Time-Series Metabolite Profiling and RNA-Seq Analysis of Chinese Hamster Ovary Cell Culture. *Sci. Rep.* **2017**, *7* (March), 1–13. https://doi.org/10.1038/srep43518.

(43) Kanda, Y. Investigation of the Freely Available Easy-to-Use Software “EZR” for Medical Statistics. *Bone Marrow Transplant.* **2013**, *48* (3), 452–458. https://doi.org/10.1038/bmt.2012.244.

(44) Ito, Y.; Terai, G.; Ishigami, M.; Hashiba, N.; Nakamura, Y.; Bamba, T.; Kumokita, R.; Hasunuma, T.; Asai, K.; Ishii, J.; Kondo, A. Exchange of

667 Endogenous and Heterogeneous Yeast Terminators in Pichia Pastoris to Tune
668 MRNA Stability and Gene Expression. *Nucleic Acids Res.* **2020**, *48* (22),
669 13000–13012. https://doi.org/10.1093/nar/gkaa1066.
670